Journal of Porphyrins and Phthalocyanines
J. Porphyrins Phthalocyanines 2017; **21**: 1–7
DOI: 10.1142/S1088424617500961

Published at http://www.worldscinet.com/jpp/

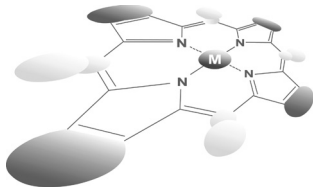

Disulfide-bridge dimeric porphyrin and their reference compounds for glutathione-based specific tumor-activation

Serkan Alpugan[a], **Derya Topkaya**[b] **and Fabienne Dumoulin**[a]*◊

[a] *Gebze Technical University, Department of Chemistry, 41400 Gebze, Kocaeli, Turkey*
[b] *Dokuz Eylul University, Department of Chemistry, Faculty of Science, 35160 Tınaztepe, Izmir, Turkey*

Received 20 December 2017
Accepted 22 December 2017

ABSTRACT: The tumor micro-environment is rich in glutathione. To exploit this feature for tumor-activatable porphyrin-based photosensitizers, a dimeric disulfide-bridged porphyrin has been designed and prepared, together with two reference derivatives, a non-cleavable dimer and a monomer. The three compounds have been investigated from a photochemical and photophysical point of view. It appears that the disulfide-bridged derivative exhibited intramolecular aggregation, but to an insufficient extent to induce a satisfying self-quenching of its photoproperties. Unlike expected, the non-cleavable dimer behaved like the monomeric derivative, due to the superior flexibility of the alkyl bridge over the disulfide bridge.

KEYWORDS: photodynamic therapy, porphyrin, tumor-activatable photosensitizer, disulfide, dimeric.

INTRODUCTION

Photodynamic therapy (PDT) is based on the conversion of molecular oxygen into its singlet toxic form at the immediate vicinity of a photosensitizer irradiated by appropriate wavelengths. The toxicity is, in theory, limited to the irradiated area (the tumor in the case of anticancer PDT). Due to its elevated metabolism compared to healthy tissues, the photosensitizer accumulates preferentially in the tumor. In any event, a varying proportion of the photosensitizer does not reach the tumor and circulates in the patient body. To avoid daylight-induced phototoxicity in healthy tissues with the remaining photosensitizer, the patient must remain in the dark until its complete excretion from the body. A way to overcome this drawback is to enhance the tumor-targeting of the photosensitizer [1], by conjugating it to antibodies [2], vitamins [3], small peptidic units [4] or more recently, to aptamers [5].

Another strategy, which is rapidly developing, takes advantage of tumors' distinctive features. In contrast with healthy tissues, tumors are more acidic [6], comprise significantly higher amounts of glutathione [7], their temperature is higher [8], specific enzymes may be overexpressed [9] and intracellular sodium ion concentration is also significantly higher (up to three times) than normal tissues [10]. On the other hand, the electronic events leading to the generation of singlet oxygen upon irradiation of the photosensitizer are quenched if the photosensitizer is aggregated (self-quenching) or in the presence of a quencher, including the protonable amine function which exerts a PET quenching effect.

This led to the development of activatable triplet photosensitizers [11], also named smart photosensitizers [12]. Dual or multiple activations may follow molecular logic gate principles. Their structure and activation mechanism is schematically represented in Fig. 1 with some examples that can be classified as follows: photosensitizer-quencher hybrids, covalent self-quenching dimeric or multimeric photosensitizers, or non-covalent self-assembled self-quenched photosensitizers: a self-assembling biarmed poly(ethylene glycol)-(pheophorbidea) 2 conjugate [13], a cell-selective glutathione-responsive tris(phthalocyanine) [14], a silicon phthalocyanine substituted axially by a pyrene for an electronic energy transfer quenching and a amino group with two methoxy-(triethylenoxy) axial chains [15], a pH and Na^+ activatable BODIPY working as an AND logic gate [16], a pH and glutathione-activatable SiPc [17], a self-assembling hence self-quenching oligoethylene glycol dendronized

◊ SPP full member in good standing

*Correspondence to: Fabienne Dumoulin, tel: +90 262 605 30 22, fax: +90 262 605 30 05, email: fdumoulin@gtu.edu.tr.

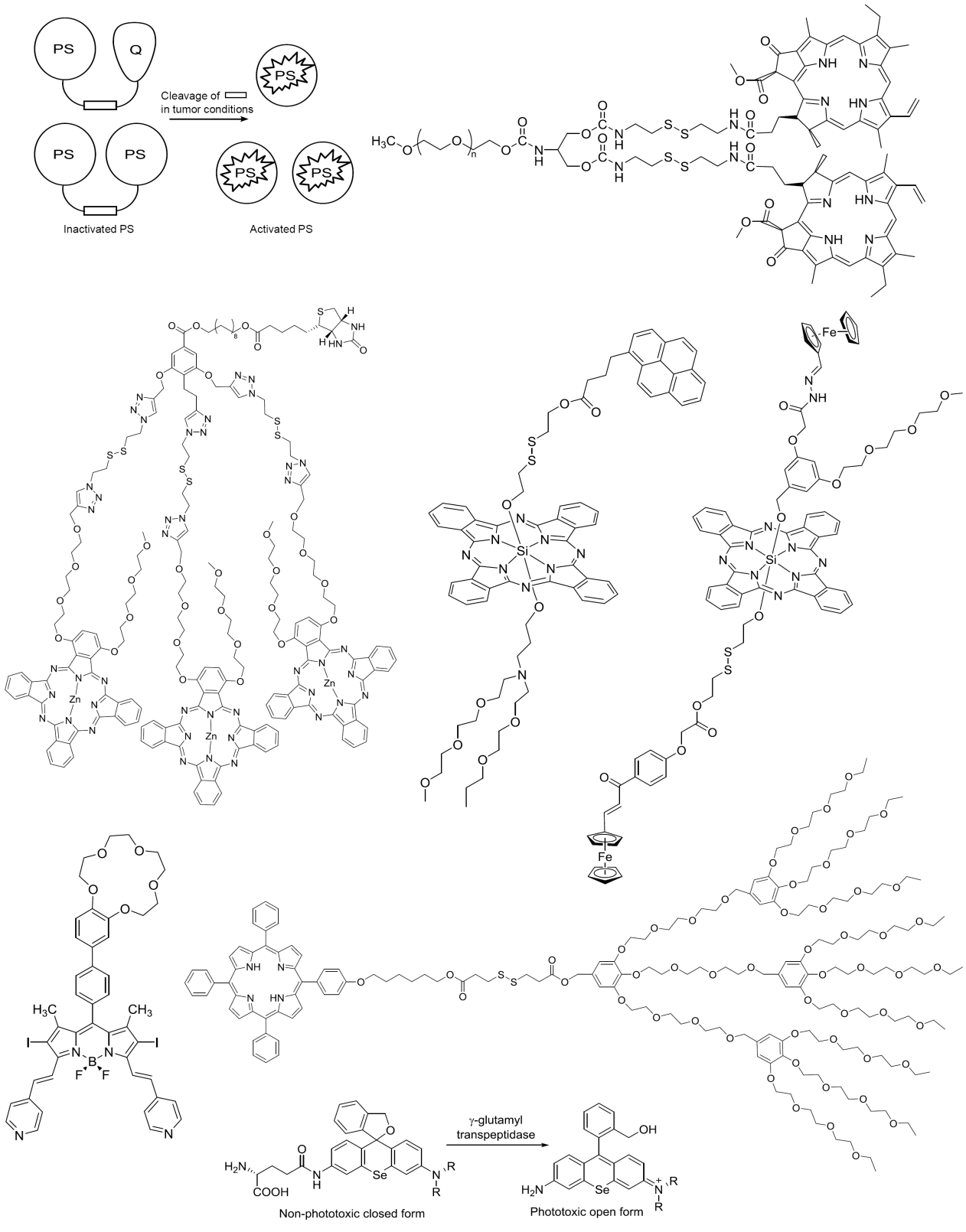

Fig. 1. Schematic representation of some previously reported tumor-specific activation of photosensitizers

reduction-sensitive porphyrins [18], a caspase 3 activatable pyropheophorbide-a molecular beacon derivative [19] and a γ-glutamyltranspeptidase activatable selenorhodamine green [20]. Unlike for phthalocyanines, and to the best of our knowledge, no porphyrin has been used for covalent self-quenching. This prompted us to explore the relevance of a disulfite-bridged dimeric porphyrin system.

RESULTS AND DISCUSSION

Molecular design

The aim of this work is to assess the relevance of using disulfide-bridged dimeric porphyrins for specific tumor-activated photosensitizers, from the point of view of a proof-of-concept. Besides, it is now known that rather than making water-soluble derivatives, often more tedious to synthesize and/or purify that hydrophobic derivatives, good formulations allow to use of hydrophobic photosensitizers for biological investigations [21]. Using the most simple tetraphenylporphyrin core was therefore decided, and the disulfide-bridged dimeric porphyrin **1** was designed. As often for such investigations, comparison with a relevant reference compound is important, and non-cleavable dimeric porphyrin **2** was designed, together with the monomeric derivative **3**. Their structures are displayed in Fig. 2.

Synthesis and characterization

Monohydroxylated porphyrin **4** [22] is the precursor for each synthesis (Scheme 1).

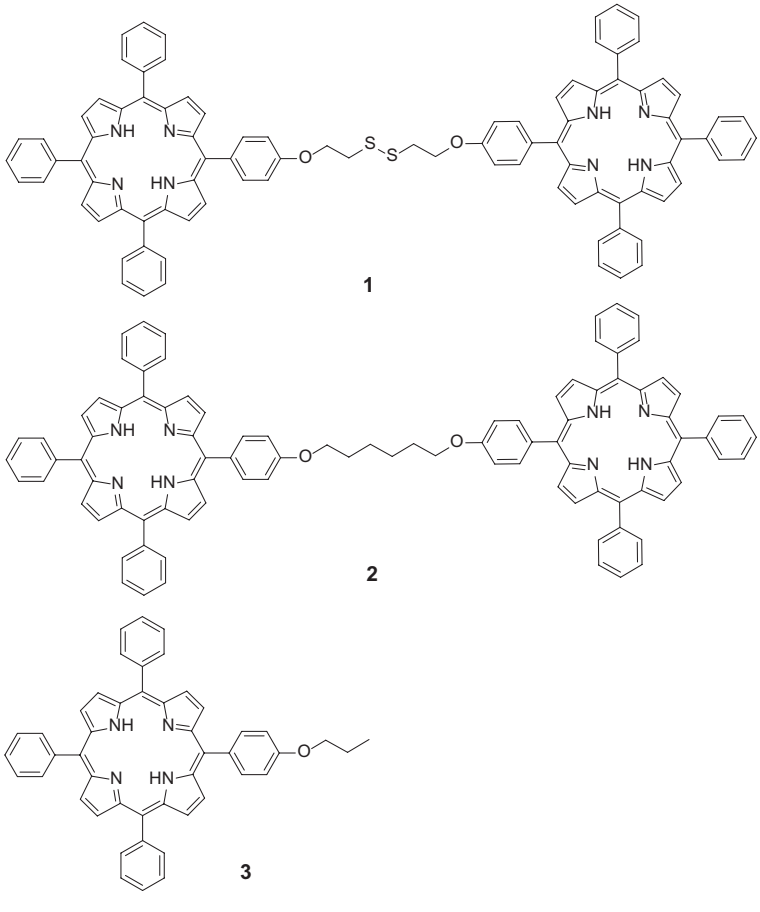

Fig. 2. Schematic representation of tumor-specific activation of photosensitiser **1** and of the reference compounds **2** and **3**

It reacts with bis-(tosylate ethyl) disulfide **5** to give **1**, with 1,6-dibromohexane to yield **2**, and with 1-bromopropane to produce **3**. One may note that unlike for reported procedures [23] and all our efforts, we managed to obtain 5 in very low yields (32% at best), and had to use it immediately after its isolation as, in our hands, it quickly decomposed. For each dimer, an excess of monohydroxylated porphyrin was used. Nonetheless, **1** was obtained in rather low yield (20%), attributed to the decomposition of 5 in the course of the reaction. With similar reagent proportions, **2** was first isolated in 10%, but could be isolated in 49% yield after optimization of the stoichiometry. The use of an excess of bromopropane for the preparation of **3** allowed its isolation in high yield (93%). All final porphyrins have been characterized by MALDI-MS, IR and ^{1}H NMR methods, which confirmed the proposed structures.

Photophysics and photochemistry

All measurements have been performed in toluene and the data are summarized in Table 1.

UV-vis absorption. The superimposed UV-vis spectra of **1**, **2** and **3** in toluene are displayed in Fig. 3a. In order to have the same amount of porphyrin core for each compound, the concentration of **1** and **2** is 5 μM, whereas the concentration of the monomeric porphyrin **3** is 10 μM. Unlike expected, only disulfide-bridged dimer **1** is aggregated as evidenced by its less sharp and less intense absorption bands. Non-cleavable dimer **2** and monomeric reference **3** have similar absorptions, hence both are non-aggregated. This is attributed to the higher flexibility of the alkyl spacer of **2**, which allows the two porphyrin cores to move quite freely, whereas the disulfide spacer is much more rigid [24], thus enhancing the self-aggregation. Self-quenching is confirmed by the linearity of the Beer–Lambert law for all compounds and in particular **1**, with no influence of the concentration (Fig. 3b). However, the self-quenching is not as considerable as one could expect for tumor specific activation, and the molar extinction coefficient of **1** is only slightly decreased compared to **2** and **3**. This was previously observed for ketal-linked dimeric phthalocyanines [25].

Fluorescence. In order to follow the cellular uptake and the subcellular localization of a photosensitizer, a slight fluorescence is useful, although it should not be too important as this may induce a lowered singlet oxygen generation (the total sum of all quantum yields being 1, with competing fluorescence and singlet oxygen generation). The aggregation of disulfide-bridge dimer **1** was not important enough to

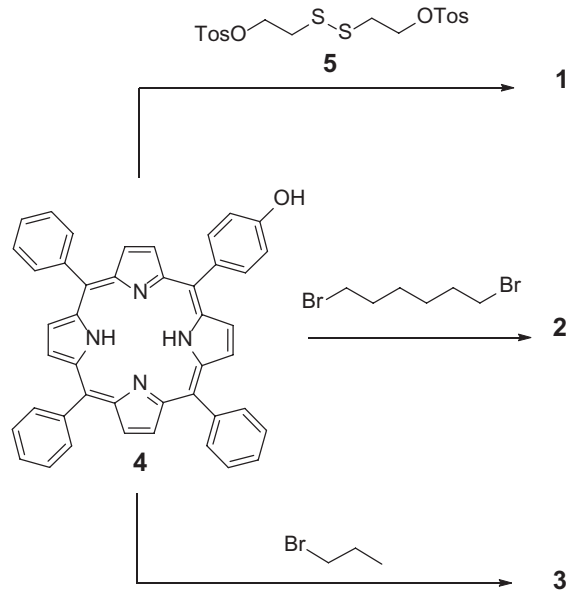

Scheme 1. Synthesis of porphyrins **1**, **2** and **3**

Table 1. Photophysical and photochemical data for **1**, **2** and **3**

	1	**2**	**3**
λ_{max} (nm)	420, 515, 550, 593, 648	420, 515, 551, 593, 649	420, 515, 551, 592, 649
ε (at 420 nm)	5.36	5.80	5.48
ϕ_F	0.15	0.15	0.15
ϕ_Δ	0.56	0.81	0.77

significantly lower fluorescence, and the quantum yields of each compound are roughly the same. Fluorescence lifetime is lower for **1** and roughly the same for **2** and **3**.

Singlet oxygen generation. Singlet oxygen generation quantum yields are, again, roughly the same for **2** and **3** (0.81 and 0.77 respectively), and much lower for the dimeric disulfide-bridged derivative **1** (Table 1 and Fig. 4). Nonetheless, with a value of 0.56, the quenching is quite weak, and unlikely to be suitable to limit the photodynamic action to the tumor micro-environment.

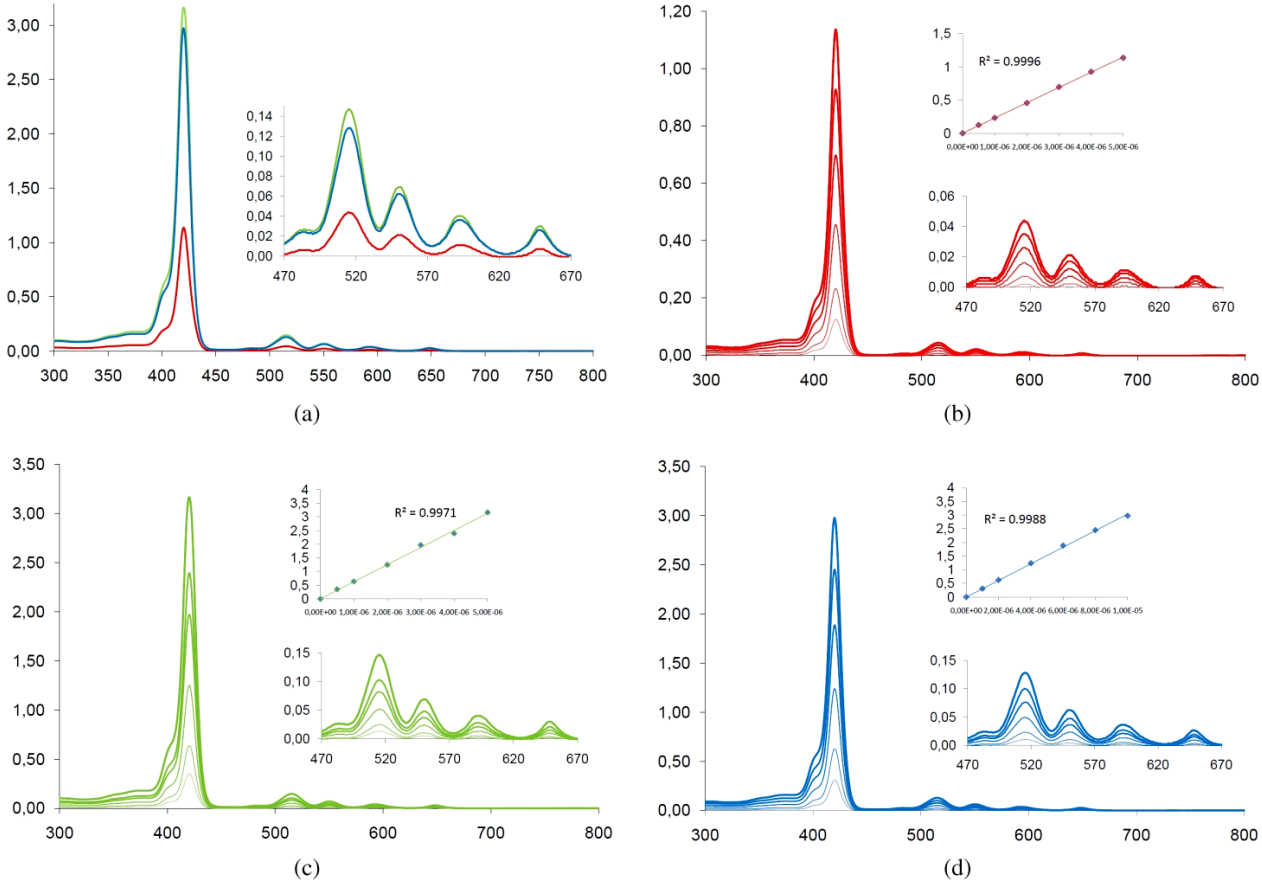

Fig. 3. (a) Superimposed UV-vis spectra of **1** (red, 5 µM), **2** (green, 5 µM) and **3** (blue, 10 µM). (b) UV-vis spectra of **1** at 0.5, 1, 2, 3, 4 and 5 µM. (c) UV-vis spectra of **2** at 0.5, 1, 2, 3, 4 and 5 µM. (d) UV-vis spectra of **3** at 1, 2, 4, 6, 8 and 10 µM. All spectra have been recorded in toluene. Abscissa: wavelength (nm). Ordinate: absorbance (a. u.)

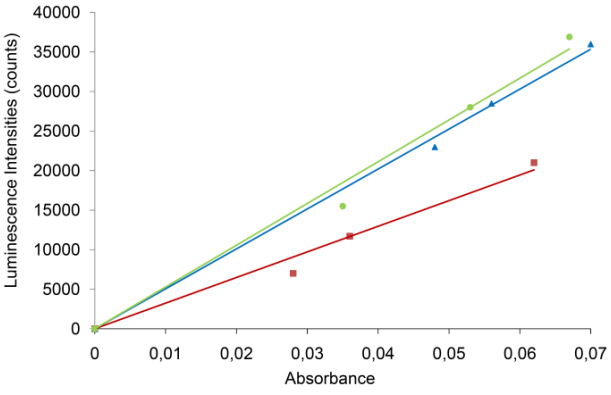

Fig. 4. Phosphorescence emission intensities of $^1O_2$ at 1270 nm *vs*. absorbance of **1** (red), **2** (green) and **3** (blue) in toluene

CONCLUSIONS AND OUTLOOK

In order to apply to porphyrin the glutathione-based tumor-environment activation of the photodynamic action, a dimeric disulfide-bridged porphyrin has been designed and prepared, together with two reference derivatives, a non-cleavable dimer and a monomer. The dimeric disulfide-bridged porphyrin was partly self-aggregated, whereas the non-cleavable dimer did not show any self-aggregation, probably due to the flexibility of the spacer. The intramolecular aggregation of the disulfide-bridged dimer was not sufficient to induce a complete self-quenching of the singlet oxygen generation. We plan next to prepare multimers with higher porphyrin contents which will be likely to exhibit better aggregation hence self-quenching outside the tumor micro-environment. This strategy was efficient with phthalocyanines [14] and is also worthy of being implemented in future works.

EXPERIMENTAL

Synthesis

Materials and methods. Monohydroxylated porphyrin **4** [22] and bis(tosylate ethyl)disulfide **5** [23] were prepared as reported. All reagents and solvents were of synthetic grade and used as received. Column chromatographies were carried out on silica gel Merck-60 (230–400 mesh, 60 A), and TLC on aluminum sheets pre-coated with silica gel 60 F254 (E. Merck). FT-IR spectra were recorded between 4000 and 480 cm^{-1} using a PerkinElmer Spectrum 100 FT-IR spectrometer. NMR spectrum were recorded in deuterated chloroform on a Varian 500 MHz spectrometer at 298 K. Mass spectra were recorded on a MALDI (matrix assisted laser desorption ionization) BRUKER Microflex LT using 2,5-dihydroxybenzoic acid (DHB) as the matrix.

***Synthesis of disulfide-bridged dimeric porphyrin* 1.** Monohydroxylated porphyrin **4** (135 mg, 0.21 mmol, 3 eq.), bis(tosylate ethyl)disulfide **5** (32 mg, 0.07 mmol, 1eq.) and K_2CO_3 (200 mg, 1.45 mmol, 20 eq.) were stirred in DMF (5 mL) overnight at room temperature, then the reaction mixture was poured into water. The resulting precipitate was filtrated, recovered in dichloromethane, dried over Na_2SO_4, and purified over silica gel column chromatography (hexane/dichloromethane, 1/1). Dark purple solid. Yield: 21% (20 mg). $C_{92}H_{66}N_8O_2S_2$, M. W. 1379.71 g/mol. FT-IR (υ, cm^{-1}): 2963, 2925, 2854, 1713, 1598, 1558, 1508, 1471, 1442, 1259, 1080, 1013, 966, 865, 792, 701, 660, 545 (S–S). ^1H NMR ($CDCl_3$, 500 MHz): δ, ppm 8.88 (s, 4H), 8.84 (s, 12H), 8.21 (d, 12H), 8.11 (d, 4H), 7.76 (d, 18H), 7.28 (s, 4H), 4.33 (t, 4H), 2.95 (t, 4H), -2.76 (s, 4H). UV-vis (toluene): λ, nm 420, 515, 550, 593, 648.

***Synthesis of non-cleavable dimeric porphyrin* 2.** Monohydroxylated porphyrin **4** (250 mg, 0.40 mmol, 4 eq.) and Cs_2CO_3 (650 mg, 2 mmol, 20 eq.) were stirred in DMF (10 mL) for 30 min at 70 °C. 1,6-dibromohexane (15 µL, 0.10 mmol, 1 eq.) was then added and the stirring continued overnight at 70 °C. The cooled reaction mixture was poured into water. The resulting precipitate was filtrated, recovered in dichloromethane, dried over Na_2SO_4 and purified over silica gel column chromatography (elution gradient, from 1/1 dichloromethane/hexane to 4/1 dichloromethane/hexane). Dark purple solid. Yield: 49% (49 mg). $C_{94}H_{70}N_8O_2$, M. W. 1343.65 g/mol. MALDI-TOF-MS (DHB): *m/z* 1344.93 (calcd. for $[MH]^+$ 1344.65). FT-IR (υ, cm^{-1}): 3315, 3053, 2947, 2854, 1596, 1559, 1058, 1470, 1441, 1401, 1350, 1246, 1214, 1174, 1074, 1016, 1001, 964, 877, 848, 796, 735, 702, 648, 578. ^1H NMR ($CDCl_3$, 500 MHz): δ, ppm 8.93 (s, 4H), 8.86 (s, 12H), 8.23 (s, 12H), 8.15 (s, 4H), 7.76 (d, 18H), 7.33 (s, 4H), 4.35 (d, 4H), 2.13 (s, 4H), 1.85 (s, 4H), -2.74 (s, 4H). UV-vis (toluene): λ, nm 420, 515, 551, 593, 649.

***Synthesis of monomeric porphyrin* 3.** Monohydroxylated porphyrin **4** (100 mg, 0.159 mmol, 1 eq.), 1-bromopropane (72 µL, 0.793 mmol, 5 eq.) and K_2CO_3 (438 mg, 3.171 mmol, 20 eq.) were stirred in DMF (5 mL) overnight at room temperature. The reaction mixture was poured into water. The resulting precipitate was filtrated, recovered in dichloromethane, and dried over Na_2SO_4. The product was purified over silica gel column chromatography (1/1 dichloromethane/hexane). Dark purple solid. Yield: 93% (100 mg). $C_{47}H_{36}N_4O$, M. W. 672.83 g/mol. MALDI-TOF-MS (DHB): *m/z* 672.93 (calcd. for $[M]^+$ 672.83). FT-IR (υ, cm^{-1}): 3318, 2963, 2925, 2853, 1597, 1559, 1507, 1472, 1441, 1400, 1349, 1259, 1221, 1175, 1017, 1016, 979, 965, 876, 846, 795, 730, 700, 658, 620. ^1H NMR ($CDCl_3$, 500 MHz): δ, ppm 8.89 (s, 2H), 8.84 (s, 6H), 8.21 (d, 6H), 8.11 (d, 2H), 7.77 (d, 9H), 7.28 (d, 2H), 4.22 (t, 2H), 2.01 (m, 2H), 1.21 (t, 3H), -2.76 (s, 2H). UV-vis (toluene): λ, nm 420, 515, 551, 592, 649.

***Synthesis of* 5.** 2-Hydroxyethyl disulfide (0.8 mL, 6.48 mmol, 1 eq.) and triethylamine (4 mL, 26 mmol, 4 eq.) were stirred in dichloromethane (20 mL) and cooled by an ice bath. Tosyl chloride (3.71g, 19.5 mmol, 3 eq.) in

dichloromethane (10 mL) was then added drop by drop, then the reaction mixture was allowed to reach room temperature and further stirred overnight. The reaction mixture was then washed by water, dried on Na_2SO_4 and quickly purified on silica gel column chromatography (eluent gradient from hexane to dichloromethane). Pale waxy liquid. 960 mg (32%). The compound is used immediately after obtaining ^{1}H NMR and FT-IR control. $C_{18}H_{22}O_6S_4$, 462.61 g/mol. FT-IR (υ, cm^{-1}): 2988, 2930, 1595, 1351, 1175, 1096, 1002, 912, 815, 756, 659, 571. ^{1}H NMR ($CHCl_3$, δ, ppm): 7.82 (d, 4H), 7.37 (d, 4H), 4.13 (t, 4H), 3.32 (t, 4H), 2.47 (s, 6H).

Photophysics and photochemistry

Absorption and fluorescence emission measurements. Absorption spectra were recorded using a Shimadzu 2101 UV-visible spectrophotometer, and fluorescence emission spectra were recorded using a Horiba FL3-2IHR in a 10 mm path length quartz cell at room temperature.

Fluorescence quantum yield determination. Fluorescence quantum yield values (ϕ_F) were calculated employing the comparative Williams' method. For this purpose, the absorbance and fluorescence spectra of the compound and of a reference standard (tetraphenylporphyrin) were measured under identical conditions. The integrated fluorescence intensities were plotted *vs.* absorbance for tetraphenylporphyrin (ϕ_F = 0.11 in toluene [26] and the studied compound. The ratio of the gradients of the plots is proportional to the quantum yield. Quantum yield (ϕ_F) values were calculated according to Eq. 1, where Grad is the gradient of the plot and *n* is the refractive index of the solvent.

$$\Phi_F = \Phi_F^{Std}\left(\frac{Grad}{Grad_{Std}}\right) \quad (1)$$

Singlet oxygen quantum yield determination. Singlet oxygen productions were measured in toluene by optical methods which are based on comparison between singlet molecular oxygen phosphorescence in the near infrared region at ~1270 nm produced by the studied compound and the reference photosensitizer tetraphenylporphyrin (Φ_Δ = 0.59 in toluene [26]. The phosphorescence signal of $^1O_2$ was recorded by Horiba–Jobin Yvon Fluorolog-3R spectrofluorimeter using a 450 W Xe arc lamp as a light source equipped with a high sensitive Hamamatsu PMT cooled housing detector (300–1700 nm). In this system, a high cut filter (1250 nm) was used in order to prevent the interference of light below 1250 nm. The absorbance and phosphorescence measurements of the studied compound and the reference photosensitizer tetraphenylporphyrin were measured at different concentrations. The phosphorescence intensities were plotted *vs*. absorbance. Singlet oxygen quantum yields (Φ_Δ) were calculated according to followed Eq. (2) using the ratio of the gradients.

$$(\phi_\Delta)_X = (\phi_\Delta)_{ST}\left(\frac{Grad_X}{Grad_{ST}}\right) \quad (2)$$

Acknowledgments

Funding from the Scientific and Technological Research Council of Turkey (TUBITAK) is acknowledged (project 214Z099).

REFERENCES

1. Moret F and Reddi E. *J. Porphyrins Phthalocyanines* 2017; **21**: 239–256.
2. Maruani A, Savoie H, Bryden F, Caddick S, Boyle RW and Chudasama V. *Chem. Commun*. 2015; **51**: 15304–15307.
3. Stallivieri A, Baros F, Jetpisbayeva G, Myrzakhmetov B, Frochot C. *Curr Med Chem.* 2015; **22**: 3185–3207.
4. Kue CS, Kamkaew A, Voon SH, Kiew LV, Chung LY, Burgess K and Lee HB. *Scientific Reports* 2016; **6**: 37209.
5. Zhu G, Niu G and Chen X. *Bioconjugate Chem.* 2015; **26**: 2186–2197.
6. Montcourrier P, Mangeat PH, Valembois C, Salazar G, Sahuquet A, Duperray C and Rochefort H. *J. Cell Sci.* 1994; **107**: 2381–2391.
7. Pendyala L, Velagapudi S, Toth K, Zdanowicz J, Glaves D, Slocum H, Perez R, Huben R, Creaven PJ and Raghavan D. *Clin. Cancer Res.* 199; **3**: 793–798.
8. Thrall DE, Page RL, Dewhirst ME, Robert E. Meyer, Hoopes PJ and Joe N. Kornegay JN. *Cancer Res.* 1986; **46**: 6229–6235.
9. Liu TW, Akens MK, Chen J, Wise-Milestone L, Wilson BC and Zheng G. *Bioconjugate Chem.* 2011; **22**: 1021–1030.
10. Cameron IL, Smith NKR, Pool TB and Sparks RL. *Cancer Res.* 1980; **40**: 1493–1500.
11. Majumdar P, Nomula R and Zhao J. *J. Mater. Chem. C* 2014; **2**: 5982–5997.
12. (a) Lovell JF, Liu TWB, Chen J and Zheng G. *Chem. Rev.* 2010; **110**: 2839–2857; (b) Li X, Kolemen S, Yoon J and Akkaya EU. *Adv. Funct. Mater.* 2017; **27**: 1604053.
13. Kim WL, Cho H, Li L, Kang HC and Huh KM. *Biomacromolecules* 2014; **15**: 2224–2234.
14. Chow SYS, Zhao S, Lo P-C, Dennis KP and Ng DKP. *Dalton Trans.* 2017; **46**: 11223–11229.
15. van de Winckel E, Schneider RJ, de la Escosura A and Torres T. *Chem. Eur. J.* 2015; **21**: 18551–18556.
16. Ozlem S and Akkaya EU. *J. Am. Chem. Soc.* 2009; **131**: 48–49.
17. Lau JTF, Lo P-C, Jiang X-J, Wang Q and Ng DKP. *J. Med. Chem.* 2014; **57**: 4088–4097.

18. Xu L, Liu L, Liu F, Li W, Chen R, Gao Y and Zhang W. *J. Mater. Chem. B*, 2015; **3**: 3062–3071.
19. Chen J, Stefflova K, Niedre MJ, Wilson BC, Chance B, Glickson JD and Zheng, G. *J. Am. Chem. Soc.* 2004; **126**: 11450–11451.
20. Chiba M, Ichikawa Y, Kamiya M, Komatsu T, Ueno T, Hanaoka K, Nagano T, Lange N and Urano Y. *Angew. Chem. Int. Ed.* 2017; **56**: 10418–10422.
21. Pucelik B, Gürol I, Ahsen V, Dumoulin F and Dabrowski JM. *Eur. J. Med. Chem*. 2016; **124**: 284–298.
22. Brookfield RL, Ellul H, Harriman A and Porter G. *J. Chem. Soc., Faraday Trans.* 2 1986; **82**: 219–233.
23. Zhang Z, Yin L, Tu C, Song Z, Zhang Y, Xu Y, Tong R, Zhou Q, Ren J and Cheng J. *ACS Macro Lett.* 2013; **2**: 40–44.
24. Alpugan S, Ekineker G, Ahsen V, Berber S, Önal E and Dumoulin F. *Crystals* 2016; **6**: 89; doi:10.3390/cryst6080089.
25. Ke M-R, Ng DKP and P-C. Lo, *Chem. Commun.* 2012; **48**: 9065–9067.
26. Figueiredo TLC, Johnstone RAW, SantAna Sørensen AMP, Burget D, Jacques P. *Photochem. Photobiol.* 1999; **69**: 517–528.